Automated image-based parameter optimization for single-pulse laser drilling

Manuel Klaiber[1,2,3], Mathias Hug[1,2,3], Lukas Schneller[1,3], Ömer Can[1], Andreas Jahn[2], Axel Fehrenbacher[2], Peter Reimann[1,4], and Andreas Michalowski[3]

[1] Graduate School of Excellence advanced Manufacturing Engineering (GSaME), University of Stuttgart, Nobelstraße 12, 70569 Stuttgart
[2] TRUMPF Laser SE, Aichhalder Straße 39, 78713 Schramberg
[3] Institut für Strahlwerkzeuge (IFSW), University of Stuttgart, Pfaffenwaldring 43, 70569 Stuttgart
[4] Institute of Parallel and Distributed Systems (IPVS), University of Stuttgart, Universitätsstraße 28, 70569 Stuttgart

Abstract A significant challenge in laser drilling is the optimization of process parameters and drilling strategies to achieve high-quality holes. This is further complicated by the fact that quality assessment is a manual and time-consuming task. This paper presents a methodology designed to significantly reduce the manual effort required in optimizing parameters for single-pulse laser drilling of 0.3 mm thick stainless steel. The objective is to precisely drill holes with an entry diameter of 70 µm and an exit diameter of 20 µm, achieving high roundness. The features of the drilled holes were extracted automatically from the raw data using a combined approach that utilizes deep learning and image processing techniques. The outcomes were compared against manual measurements. Results indicate that the mean deviations between automated and manual measurements for both inlet and outlet diameters are less than one micrometer. We employed a Bayesian optimization algorithm to efficiently explore the parameter space without the need for incorporating expert knowledge. The approach rapidly identified optimal drilling parameters after only a few iterations, significantly expediting the optimization process and considerably reducing manual labor.

Keywords Laser drilling, semantic segmentation, feature extraction, Bayesian optimization

DOI: 10.58895/ksp/1000174496-1 erschienen in:
Forum Bildverarbeitung 2024
DOI: 10.58895/ksp/1000174496 | https://www.ksp.kit.edu/site/books/m/10.58895/ksp/1000174496/

1 Introduction

The manufacturing industry is constantly searching for advanced methods to improve the precision and efficiency of laser drilling processes [1]. Various strategies have been employed, including traditional methods such as Design of Experiments (DoE) and Response Surface Methodology (RSM), as well as advanced computational techniques. For example, Gupta et al. [2] used DoE and RSM to optimize the hole quality in ms-pulsed laser drilling, while Wang et al. [3] applied artificial neural networks to predict optimal drilling parameters for ns-pulsed laser drilling in stainless steel. Chatterjee et al. [4] used neuro-fuzzy systems and genetic programming to predict drilling outcomes, showing reasonable accuracy. However, these strategies often require extensive experimental setups or training data and cannot efficiently navigate complex parameter spaces to search for optimal drilling parameters.

Recent advances in computational techniques, particularly approaches to Bayesian optimization (BO), provide a promising alternative that can predict multi-dimensional parameters spaces in laser processes with significantly fewer iterations and less manual intervention [5]. Yang et al. [6] applied BO to improve taper and drilling time in spiral drilling of stainless steel, achieving suitable results with few iterations. Bamoto et al. [7] optimized a femtosecond laser micro-drilling process and Menold et al. [8] demonstrated the versatility of BO in optimizing laser cutting, laser welding and laser polishing and showed that less experiments are needed than with traditional approaches.

In addition to the actual optimization of drilling parameters, the extraction of the features required by the optimization approaches represents a significant challenge in process optimization. In previous studies on laser drilling, the quality measurements were predominantly assessed through manual measurements [2]. Feuer et al. [9] propose an automated approach to extract the drilling geometry as features. Approaches to automated feature extraction and quality control for a laser welding process using semantic segmentation are presented by Hartung et al. [10].

This paper presents an approach that incorporates sophisticated feature extraction techniques that employ a combination of deep learning models and conventional image processing methods to accurately ex-

tract quality features of single-pulse drilled holes. Subsequently, this study investigates the potential of BO with the aim of determining optimal laser parameters including pulse power, pulse length, and focus position to ensure high-quality holes in terms of diameter and roundness.

2 Materials and Methods

This section describes the experimental setup for single-pulse laser drilling of thin metal sheets. Furthermore, it gives an overview of the feature extraction and parameter optimization methods utilized. The procedure of the iterative optimization process is shown in Figure 1. For the first n=6 optimization steps, the parameter sets are generated using a sobol sequence to ensure that the points are evenly distributed in the parameter space. Subsequent parameter sets are suggested by the BO.

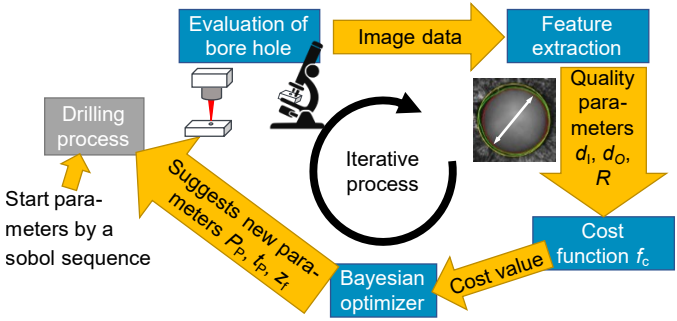

Figure 1: Optimization process with a Bayesian Optimizer.

2.1 Experimental Setup

Figure 2 shows the experimental setup of the single-pulse laser drilling process. In this study, a continuous wave (cw) single mode fiber laser (TRUMPF TruFiber 2000) was used to perform the single-pulse laser drilling experiments. The emission wavelength of the unpolarized laser

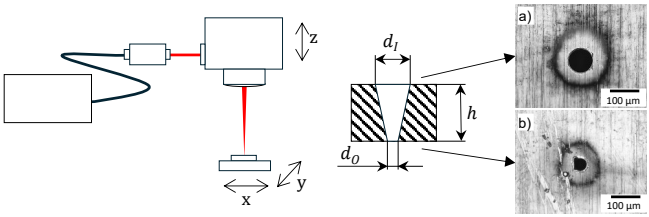

Figure 2: Left: Experimental Setup. Right: Borehole cross section with images of an a) inlet with diameter d_I and b) outlet with diameter d_O.

was specified as 1075 nm in conjunction with a beam propagation factor of M^2<1.2. The laser beam was positioned onto the stainless steel sample with a galvanometer scanner. A telecentric F-Theta lens with a focal length of 163 mm was used, resulting in a focus diameter ($1/e^2$) of d_f= 20 µm. The pulsed operation mode of the laser source enables the generation of pulses with a peak power P_P up to 1400 W. This allows for the adjustment of the pulse duration between values from 1 to 25 µs. The setup was equipped with linear stages (x,y) for the sample and a linear drive (z) for the process optics to adjust the focus position. The focus position can thus be positioned with an accuracy of one micrometer.

The materials used for the experiments are stainless steel (1.4310) substrates. The substrates, with a thickness h of 0.3 mm, were cut to a size of 100 mm × 50 mm. An optical microscope (Zeiss Axio Imager) was used to evaluate the borehole criteria, such as inlet (Figure 2 a) and outlet (Figure 2 b). A 20× magnification was used for optical microscopic observation, where one pixel is equivalent to 0.172 × 0.172 µm^2. The evaluation criteria include the diameter of the inlet d_I and of the outlet d_O, as well as the roundness R of the outlet. We drilled and analyzed i=3 holes per parameter set to reduce the influence of side effects from the inherent noise of laser processing and other uncertainties.

2.2 Feature Extraction

The objective is to automatically extract the features that are required for the parameter optimization directly from the microscope images. The features include the borehole's inlet diameter d_I and outlet diame-

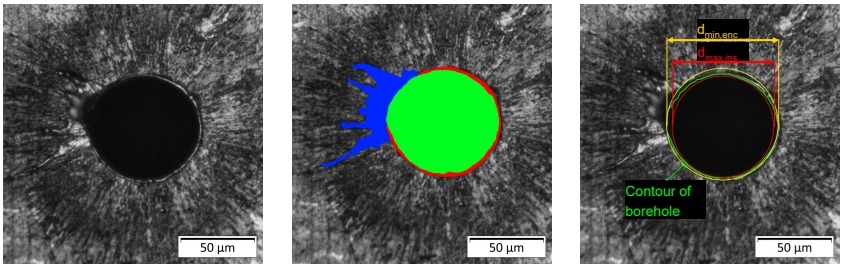

Figure 3: (a) Inlet of a borehole with breakthrough. (b) Segmented classes by the neural network: melt (blue), burr (red) and borehole with breakthrough (green). (c) Contour of the borehole (green) from which the diameter of the maximum inscribing circle $d_{max,ins}$ (red) and the diameter of the minimum enclosing circle $d_{min,enc}$ (yellow) were derived.

ter d_O, the borehole's roundness R, the area of the melt deposits around the borehole, and a classification of whether a breakthrough has occurred. Initial attempts to perform feature extraction based solely on conventional image processing methods have not delivered satisfactory results. Due to the divergent surface properties of the materials to be processed, there is a high degree of variance in the captured images, e.g., due to reflections and mirroring. This variance requires great efforts to manually adjust the algorithm parameters of conventional image processing methods. Deep learning methods represent another viable approach to address natural deviations in images like reflections and mirroring. Nevertheless, a method based exclusively on deep learning that directly determines quality characteristics is intricate and challenging for the operator to comprehend. A combined approach, comprising semantic segmentation models and conventional image processing methods, enables a more robust and understandable extraction of features. In our study, we employ two semantic segmentation models, each with a neural network architecture modified from the SDU-net [11]. These models are used to segment images from the top (inlet) and bottom (outlet) of the borehole. The inlet model classifies the image into the following classes, as partly shown in Figure 3(b): *burr*, *melt*, and one of the classes *borehole with breakthrough* or *borehole*

without breakthrough. The outlet model segments the image into: *background*, *melt*, *borehole with breakthrough*, and *borehole without breakthrough*. To train the inlet model, 68 labeled images were used, while the outlet model was trained with 44 images. The discrepancy in the number of training images is due to the fact that only continuous boreholes are included in the outlet dataset. The models are initialized randomly without any pre-training. Both models use *Categorical Focal Loss* [12] as loss function. The classes segmented by the models are further analyzed using conventional image processing methods. Figure 3(c) shows, how the borehole diameter d_I was calculated using the contour (green) of the segmented borehole class *borehole with breakthrough*. This calculation involves averaging the diameters of two specific circles: the minimum enclosing circle, $d_\mathrm{min,enc}$ (shown in yellow), determined using the method proposed by Welzl et al. [13], and the maximum inscribing circle, $d_\mathrm{max,ins}$ (shown in red), as described by Xia et al. [14].

The roundness R of the borehole is defined by the ratio of the borehole area A_borehole (Figure 3(b) green) to the area of the minimum enclosing circle $A_\mathrm{min,enc}$ [15]. The melt deposition area is calculated as the sum of the segmented burr and melt area classes. In order to ascertain whether breakthrough is present, the areas belonging to the *borehole with breakthrough* and *borehole without breakthrough* classes are compared. The classification of breakthrough is dependent on the class from which the larger area was segmented.

2.3 Bayesian Optimization

To optimize the single-pulse laser drilling process, we used the extracted data in a Bayesian Optimization framework. The goal was to find laser parameters that yield high-quality holes with defined geometries. The AX Service API [16] was used, with a Gaussian Process as a surrogate model [17], and the default squared exponential kernel for the optimization. This approach efficiently explored the parameter space, aiming to optimize the drilling process with minimal experimental effort. As acquisition function *Expected Improvement* [18] was used. More detailed explanations and applications of the BO for other laser processes were given by Menold et al. [8]. Table 1 shows the process parameters that were varied and the quality parameters that result from the feature extraction process described in Section 2.2. The area

of the melt was excluded from the BO to concentrate on enhancing the accuracy of the diameters and roundness.

Table 1: Parameters and variables for the process.

Category	Parameter/Variable	Symbol	Value Range, Target
Process Parameters	Pulse Power	P_P	300 W ... 1400 W
	Pulse Length	t_P	1 µs ... 25 µs
	Focal Position	z_f	-200 µm ... 200 µm
Quality Variables	Inlet Diameter	d_I	$d_\mathrm{I,target} = 70\,\mu\mathrm{m}$
	Outlet Diameter	d_O	$d_\mathrm{O,target} = 20\,\mu\mathrm{m}$
	Roundness	R	0 ... 1, R_target=1

For each parameter set, i=3 holes were drilled and evaluated with an optical microscope. The image data was analyzed by feature extraction to obtain the inlet and outlet diameters $d_\mathrm{I}, d_\mathrm{O}$ and the roundness R of the outlet. The cost function

$$\begin{aligned} C(x) = {} & w_\mathrm{d,I} \cdot |d_\mathrm{I}(x) - d_\mathrm{I,target}| + w_\mathrm{d,O} \cdot (d_\mathrm{O}(x) - d_\mathrm{O,target})^2 \\ & + w_\mathrm{R} \cdot (1 - R(x)) + w_\mathrm{E} \cdot E_\mathrm{P} \end{aligned} \tag{1}$$

with the process parameters x=($P_\mathrm{P}, t_\mathrm{P}, z_\mathrm{f}$) and the weights $w_\mathrm{d,I}$=1 µm^{-1}; $w_\mathrm{d,O}$=4 µm^{-1}; w_R=200; w_E=2 mJ^{-1} calculates the cost C of each borehole, with lower costs indicating higher quality. Determining the appropriate weights w requires domain-specific expertise and is inherently subjective. These weightings are contingent upon the optimization objectives and the relative magnitude of the associated process parameters. Given the significant impact of these weightings on the optimization outcomes, it may be necessary to adjust them prior to initiating the optimization process. $C(x)$ is formulated to achieve a target inlet and outlet diameter with maximum roundness of the outlet. Pulse length and pulse power were summarized as pulse energy E_P=$P_\mathrm{P} \cdot t_\mathrm{P}$, which is to be minimized to encourage a short drilling duration and lower heat input. If no breakthrough occurs, the cost C becomes high due to the quadratic influence of the outlet diameter term $w_\mathrm{d,O} \cdot (d_\mathrm{O}(x) - d_\mathrm{O,target})^2$. In addition, the roundness R is set to zero, which leads to maximum costs of the roundness term $w_\mathrm{R} \cdot (1 - R(x))$=200.

3 Results and Discussion

This section discusses the results obtained from the feature extraction techniques, which are divided into two parts: The evaluation of the training of the segmentation networks and the evaluation of the feature extraction methods based on the segmentation results. Subsequently, we explore the findings from the BO process.

3.1 Results of the Feature Extraction

To evaluate the effectiveness of the feature extraction process, 80 images of borehole openings, captured from 40 laser-drilled boreholes (40 images of inlets and 40 images of outlets), have been labeled by experts and are available for analysis. These images were not included in the training data set. We employ the Intersection over Union (IoU) [19] as evaluation metric to assess the model predictions:

$$\mathrm{IoU}(A, B) = \frac{|A \cap B|}{|A \cup B|} \tag{2}$$

Where A is the segmentation mask used for training and B is the prediction of the segmentation network. During the evaluation, the inlet model achieved an IoU value of 0.97 for the borehole classes, while the outlet model achieved an IoU value of 0.95 for this class. However, the melt and burr classes exhibit a decline in performance, with each reaching an IoU value of 0.75. This is primarily attributable to the distinctive characteristics of the melt, which also manifests as a maximum IoU value of 0.78 for these two classes during training.

After the image segmentation, the diameters are calculated based on the prediction of the borehole models. To assess the precision of the measurement techniques with respect to representative data, the inlets and outlets of 40 additional boreholes, drilled in identical experimental conditions as illustrated in Figure 2, were evaluated. Figure 4 shows the diameters based on automatic feature extraction $d_{\text{feat. extr.}}$ (x-axis) and manual measurements $d_{\text{man.}}$ (y-axis) of the inlet (blue) and outlet (green). The manual measurements were conducted using an optical microscope. The right side of Figure 4 shows the deviation between the feature extraction diameter and the manual measurement. The mean deviation is -0.5 µm for the inlet and 0.34 µm for the outlet,

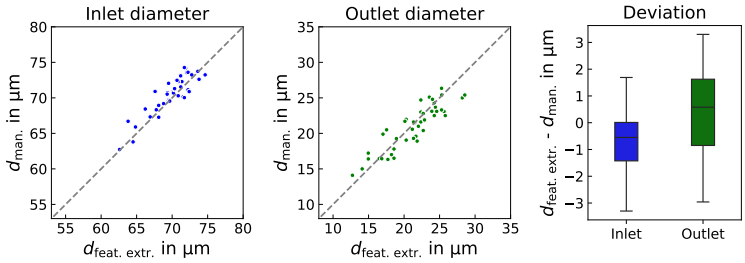

Figure 4: Comparison of the results of automatic feature extraction (x-axis) with manual measurements (y-axis) of inlet and outlet diameters.

which is within the expected accuracy and tolerance limits for borehole measurements. These low deviations, typical between automated and manual measurement techniques, validate the effectiveness of feature extraction in determining inlet and outlet diameters. The methods outlined enable automated borehole measurement, facilitating the use of the extracted features for parameter optimization and significantly reducing manual effort.

3.2 Results of the Bayesian Optimization

Figure 5 shows the evolution of the process parameters (left) and quality variables (right) during the optimization process. During the initialization process (orange) with parameters chosen by the sobol sequence, a wide range of process parameters is covered, resulting in a high cost value (red curve). In the start sequence, three parameter sets n=3, 4, 5 did not lead to through holes, because the pulse duration was too short. In the following optimization steps the BO suggested only one more parameter set at n=26, where no breakthroughs were achieved. In the bottom right of Figure 5 the inlet and outlet of the borehole with the minimum cost value C_{12}=$86.00^{+13.57}_{-20.83}$ after n=12 iterations with process parameters z_f=-79.0 µm, P_L=898 W and t_P=17 µs is shown. This led to an inlet diameter of d_I=$68.0^{+0.5}_{-0.8}$ µm, an outlet diameter of d_O=$18.03^{+0.57}_{-0.43}$ µm and a roundness of R=$0.84^{+0.6}_{-0.4}$ µm which are close to the targeted values.

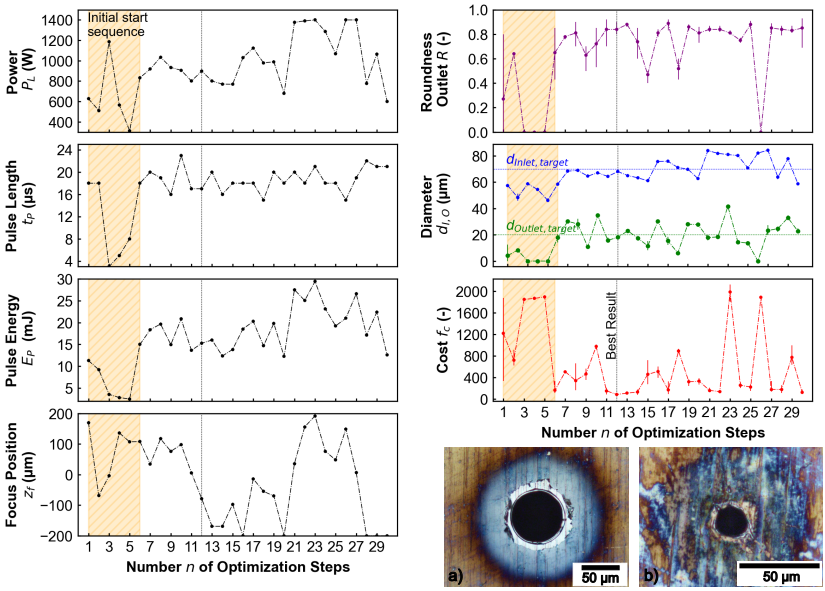

Figure 5: Evolution of the process parameters (left) and quality variables (right) of the drilled holes and the value of the cost function during optimization (red). The error bars are min/max values of three experiments for each parameter set. a) inlet and b) outlet of borehole n=12.

4 Conclusion

The aim of this work was to reduce the manual effort in parameter search for single-pulse laser drilling. By employing a combination of deep learning techniques for the segmentation of microscope images and conventional image processing methods for the measurement of segmentations, it is possible to perform a robust and rapid determination of the quality features of a borehole, particularly in challenging imaging situations, such as those caused by reflections. The results demonstrate that the mean deviations between manual measurements and feature extraction for both inlet and outlet diameters are less than one micrometer. Furthermore, BO has been demonstrated to be an effective approach for achieving target hole characteristics with a min-

imal number of iterations. In an optimization experiment comprising 30 iterations, the parameters conducive to drilling with the desired characteristics were identified after just 12 iterations. This significantly reduces the need for traditional full-factorial experimental designs, simplifying the laser drilling optimization process and increasing efficiency in industrial applications.

References

1. Y. C. Shin, B. Wu, S. Lei, G. J. Cheng, and Y. Lawrence Yao, "Overview of Laser Applications in Manufacturing and Materials Processing in Recent Years," *Journal of Manufacturing Science and Engineering*, vol. 142, no. 11, p. 110818, 10 2020.
2. A. K. Gupta, R. Singh, and D. Marla, "Millisecond pulsed laser microdrilling of stainless steel – optimizing hole quality using response surface methodology," *Journal of Laser Micro/Nanoengineering*, 2023.
3. C.-S. Wang, Y.-H. Hsiao, H.-Y. Chang, and Y.-J. Chang, "Process parameter prediction and modeling of laser percussion drilling by artificial neural networks," *Micromachines*, vol. 13, no. 4, 2022.
4. S. Chatterjee, S. S. Mahapatra, V. Bharadwaj, B. N. Upadhyay, and K. S. Bindra, "Prediction of quality characteristics of laser drilled holes using artificial intelligence techniques," *Engineering with Computers*, vol. 37, no. 2, pp. 1181–1204, 2021.
5. A. Michalowski, A. Ilin, A. Kroschel, S. Karg, P. Stritt, A. Dais, S. Becker, G. Kunz, S. Sonntag, M. Lustfeld, P. Tighineanu, V. Onuseit, M. Haas, T. Graf, and H. Ridderbusch, "Advanced laser processing and its optimization with machine learning," 03 2023, p. 4.
6. J. Yang, J. Niu, L. Chen, K. Cao, T. Jia, and H. Xu, "Tunable simultaneous Bayesian optimization of hole taper and processing time in qcw laser drilling," *Journal of Manufacturing Processes*, vol. 109, pp. 471–480, 2024.
7. K. Bamoto, H. Sakurai, S. Tani, and Y. Kobayashi, "Autonomous parameter optimization for femtosecond laser micro-drilling," *Opt. Express*, vol. 30, no. 1, pp. 243–254, Jan 2022.
8. T. Menold, V. Onuseit, M. Buser, M. Haas, N. Bär, and A. Michalowski, "Laser material processing optimization using bayesian optimization: A generic tool," *Light: Advanced Manufacturing*, 2024.

9. A. Feuer, R. Weber, R. Feuer, D. Brinkmeier, and T. Graf, "High-quality percussion drilling with ultrashort laser pulses," *Applied Physics A*, vol. 127, no. 9, 2021.
10. J. Hartung, A. Jahn, and M. Heizmann, "Quality control of laser welds based on the weld surface and the weld profile."
11. S. Wang, S.-Y. Hu, E. Cheah, X. Wang, J. Wang, L. Chen, M. Baikpour, A. Ozturk, Q. Li, S.-H. Chou, C. D. Lehman, V. Kumar, and A. Samir, "U-net using stacked dilated convolutions for medical image segmentation."
12. M. Yeung, E. Sala, C.-B. Schönlieb, and L. Rundo, "Unified focal loss: Generalising dice and cross entropy-based losses to handle class imbalanced medical image segmentation," *Computerized medical imaging and graphics : the official journal of the Computerized Medical Imaging Society*, vol. 95, p. 102026, 2022.
13. E. Welzl, "Smallest enclosing disks (balls and ellipsoids)," in *New Results and New Trends in Computer Science*, ser. Lecture Notes in Computer Science, H. Maurer, Ed. Heidelberg: Springer-Verlag, 1991, vol. 555, pp. 359–370.
14. R. Xia, W. Liu, J. Zhao, H. Bian, and F. Xing, "Robust algorithm for detecting the maximum inscribed circle," in *Proc. of the 10th IEEE International Conference on Computer-Aided Design and Computer Graphics*. IEEE, 2007, pp. 230–233.
15. B. Walters, T. Uynuk-Ool, M. Rothdiener, J. Palm, M. L. Hart, J. P. Stegemann, and B. Rolauffs, "Engineering the geometrical shape of mesenchymal stromal cells through defined cyclic stretch regimens," *Scientific reports*, vol. 7, no. 1, p. 6640, 2017.
16. E. Bakshy, L. Dworkin, B. Karrer, K. Kashin, B. Letham, A. Murthy, and S. Singh, "Ae: A domain-agnostic platform for adaptive experimentation," Red Hook, NY, USA, 2018.
17. C. E. Rasmussen, *Gaussian processes for machine learning*, ser. Adaptive computation and machine learning. Cambridge, Mass.: MIT Press, 2006.
18. J. Mockus, V. Tiesis, and A. Zilinskas, "The application of Bayesian methods for seeking the extremum," *Towards Global Optimization*, vol. 2, no. 117-129, p. 2, 1978.
19. P. Jaccard, "Lois de distribution florale dans la zone alpine," *Bulletin de la Societe Vaudoise des Sciences Naturelles*, vol. 38, no. 144, pp. 69–130, 1902.